

# Decorated Amyloid Fibril Morphology is Controlled by the Conformation and Position of the Displayed Protein.

Christopher J. Forman,<sup>†</sup> Adrian A. Nickson,<sup>†</sup> Spencer Anthony-Cahill,<sup>‡</sup> Andrew J.  
Baldwin,<sup>†</sup> Gillian Kaggwa,<sup>¶</sup> Urs Feber,<sup>¶</sup> Khizar Sheikh,<sup>¶</sup> Suzanne Jarvis,<sup>¶</sup> and  
Paul D. Barker<sup>\*,†</sup>

*Department of Chemistry, University of Cambridge, Lensfield Road, Cambridge, CB2 1EW, UK,  
Department of Chemistry, Western Washington University, Bellingham, WA 98225-9150, USA,  
and UCD Conway Institute of Biomolecular and Biomedical Research, University College  
Dublin, Belfield, Dublin 4 Ireland*

E-mail: pdb30@cam.ac.uk

## Supporting Information

---

\*To whom correspondence should be addressed

<sup>†</sup>deptChem

<sup>‡</sup>WWU

<sup>¶</sup>UCD

## Fusion Protein Sequences

Name	Sequence	$M_w$	Number of Residues
Cytochrome $b_{562}$	ADLEDNMETLNDNLKVIEKA DNAAQVKDALTKMRAAALDA QKATPPKLEDKSPDSPEMKD FRHGF DILVGQIDDALKLNE GKVKEAQAAAEQLKTTRNAY HQKYR	11780.2	106
SH3	GSMSAEGYQYRALYDYKKER EEDIDLHLGDILTVNKGSLV ALGFSDGQEAKPEEIGWLNG YNETTGERGDFPGTYVEYIG RKKISP	9638.6	86
SS	SH3 – GGGGSGGGGS – SH3	19925.7	182
SSB	SH3 – GGGGSGGGGS – SH3 – GSGGGG – Cyt $b_{562}$	32096.2	294
SSSB	SH3 – GGGGSGGGGS – SH3 – GGGGSGGGGS – SH3 – GSGGGG – Cyt $b_{562}$	42383.3	390
BSS	Cyt $b_{562}$ – GSSRLVPR – SH3 – GGGGSGGGGS – SH3	32576.9	296
BSSB	Cyt $b_{562}$ – GSSRLVPR – SH3 – GGGGSGGGGS – SH3 – GSGGGG – Cyt $b_{562}$	44639.5	408

## Recurring Motifs

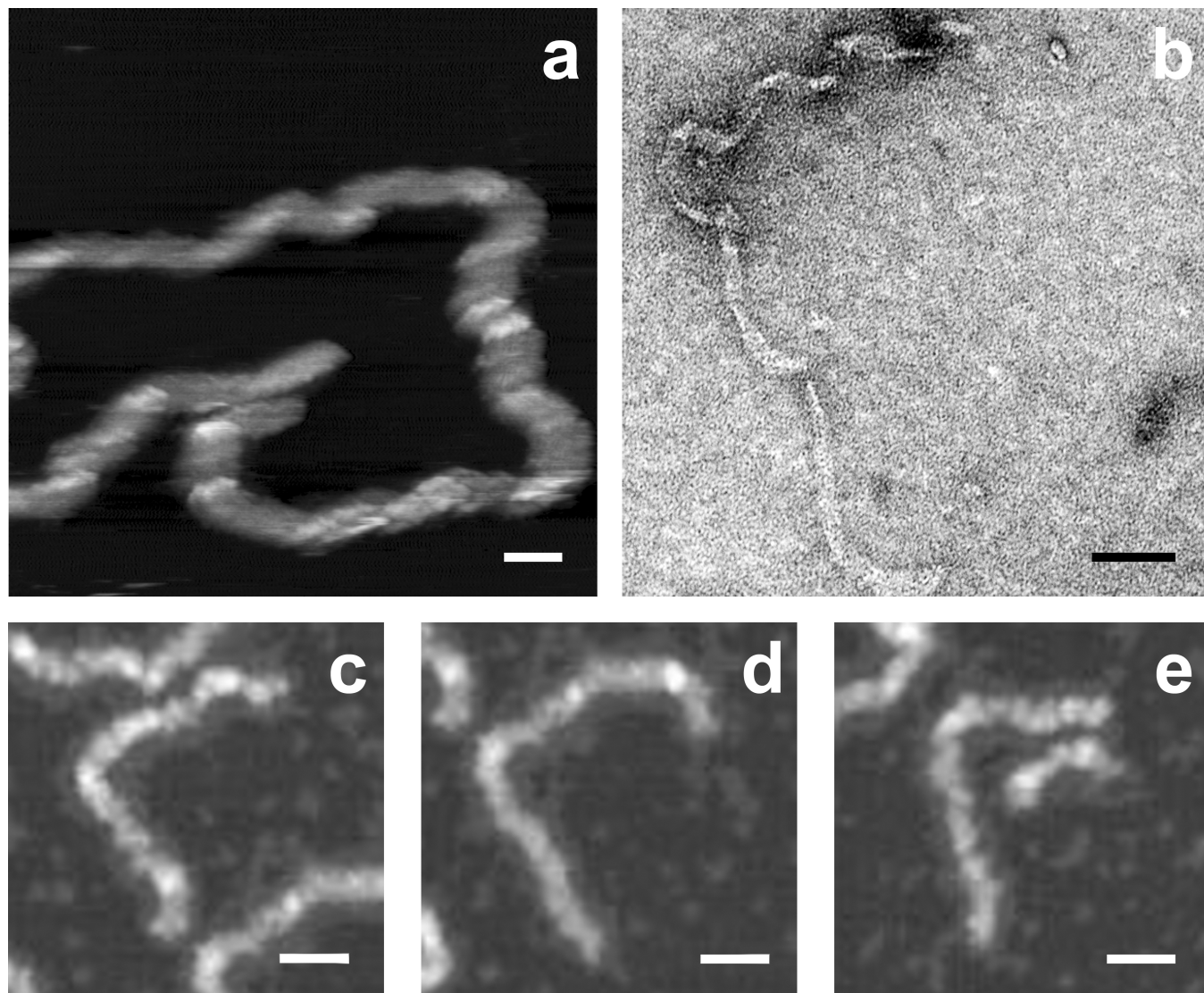


Figure 1: The L-shaped fibre motif appears in three very different situations. **(a)** AFM of SSB holo-fibre on a mica substrate using high resolution AFM in a liquid environment. **(b)** TEM of BSS apo-fibre, on a carbon film, negatively stained with uranyl acetate in high vacuum. **(c, d, e)** Low resolution AFM of BSS 0% fibre on mica substrate in air. These three different fibres (actually digitally magnified subsets of Figure 2c in the main text) exhibit almost identical L-shape formations.

The simplest possible shape for a kinked fibre is an L-shape which has occurred frequently throughout this investigation. Figure 1 depicts a series of images of different fibre types taken using different techniques on distinct substrates in a variety of environments: air, liquid and vacuum. The L-shaped motif is apparent in all of them (in one case, several times in succession), which settles

long standing questions about the validity of comparing fibres in radically environments.

Different segments of the holo-SSB fibre, acquired in liquid on a mica substrate, in Figure 1a. There is a substantial difference in morphology of the different segments of the fibre. While some of the details in the features are due to tip artifacts, the fundamental period of the underlying helix is shorter on the right edge than it is on either the top or bottom edges. Scanning at 45 degrees confirmed this observation.

Figure 1b presents a TEM image of a BSS apo-fibre on a carbon support film in vacuum and clearly reveals differing periodicity on each segment of the L-shape. That the change of morphology within the fibre occurs at the same position as the change in direction of the principal axis is entirely consistent with a change in alignment of filament registry.

Figures Figure 1c,d and e are all BSS apo-fibres seen by low resolution AFM on mica in air. The similarity of the angle between the segments is striking — particularly given the completely different surrounding fibres in each case. Any changes in periodicity are less apparent.

## Additional AFM Data

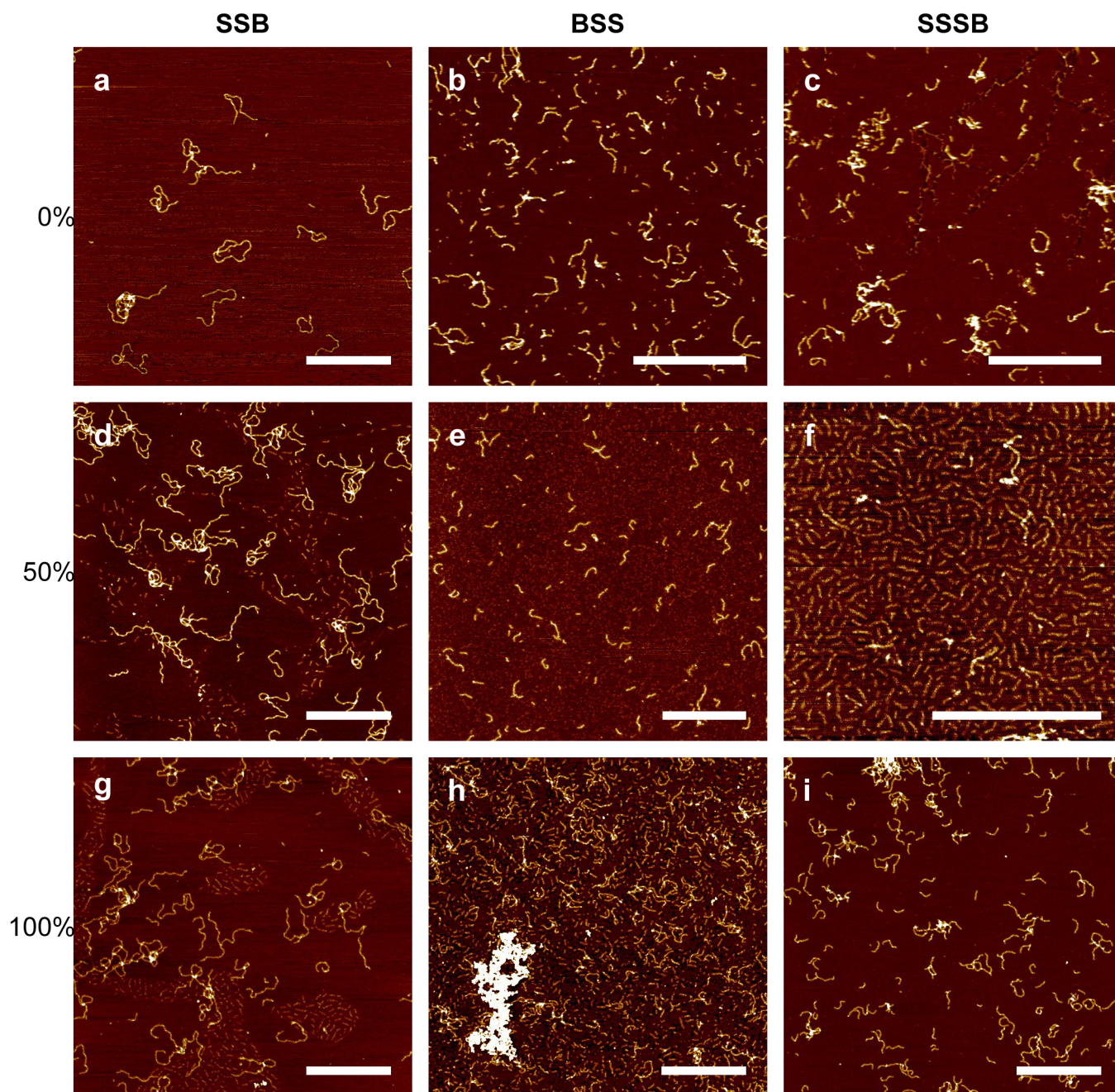


Figure 2: Supporting AFM data. Left to Right: SSB, BSS and SSSB. Top to bottom: fibres taken from solutions of 0%, 50% and 100% heme to protein ratio. Note the clustering of the fragments and the fact that the fragments never touch each other. In some a cases a faint layer of material between the fragments can be seen.

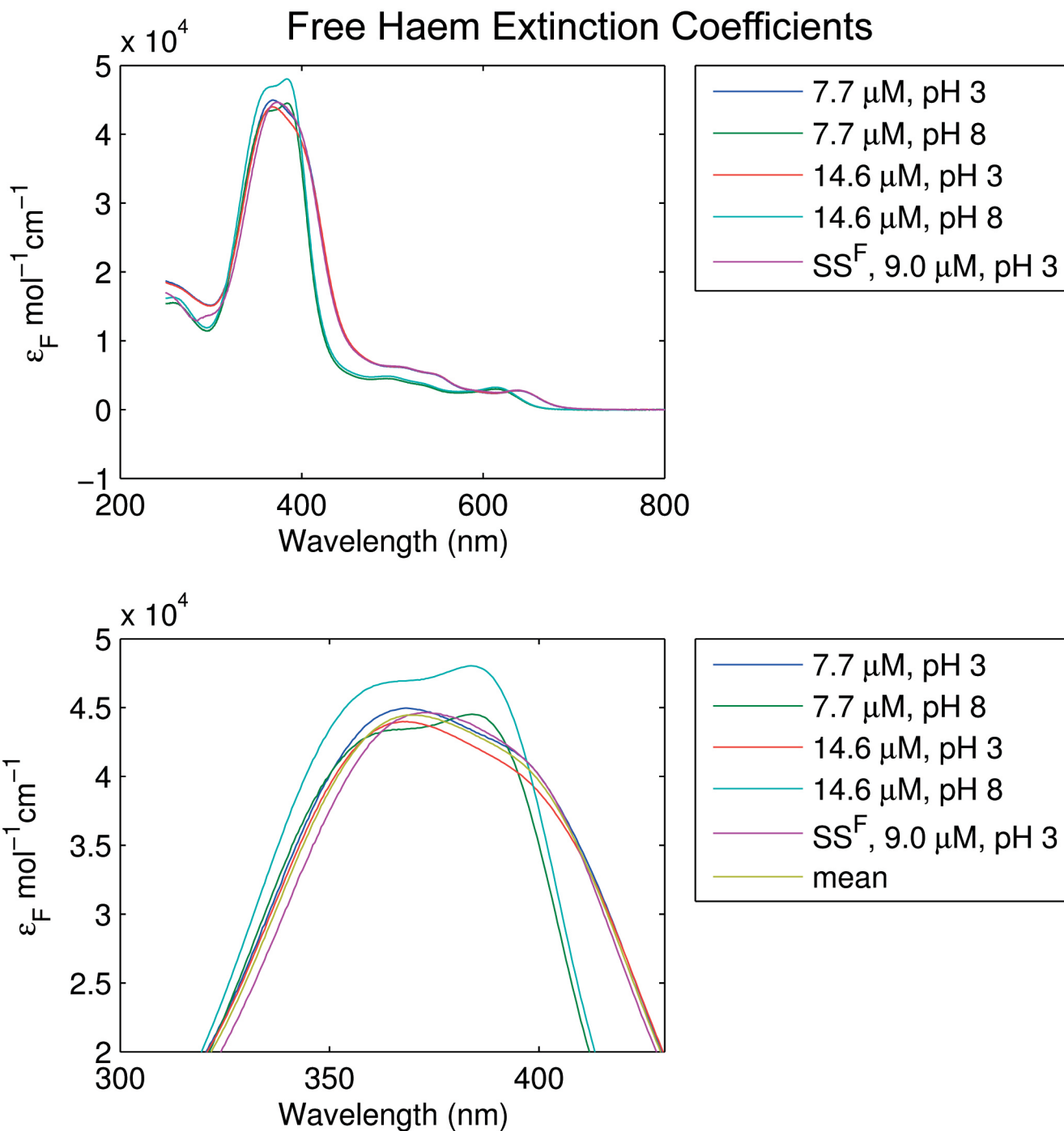


Figure 3: The extinction coefficients of free heme at a variety of concentrations and conditions in a solution of 0.1 M Tris HCl at pH 8 and 1 mM HCl at pH 3. This information is necessary to deconvolve the spectra arising from performing the heme titrations at pH 3. The acidic pH is required to keep the fibres intact. The set of means values was used in the spectral analysis. The lower image is a digital magnification of the peaks in the upper image.

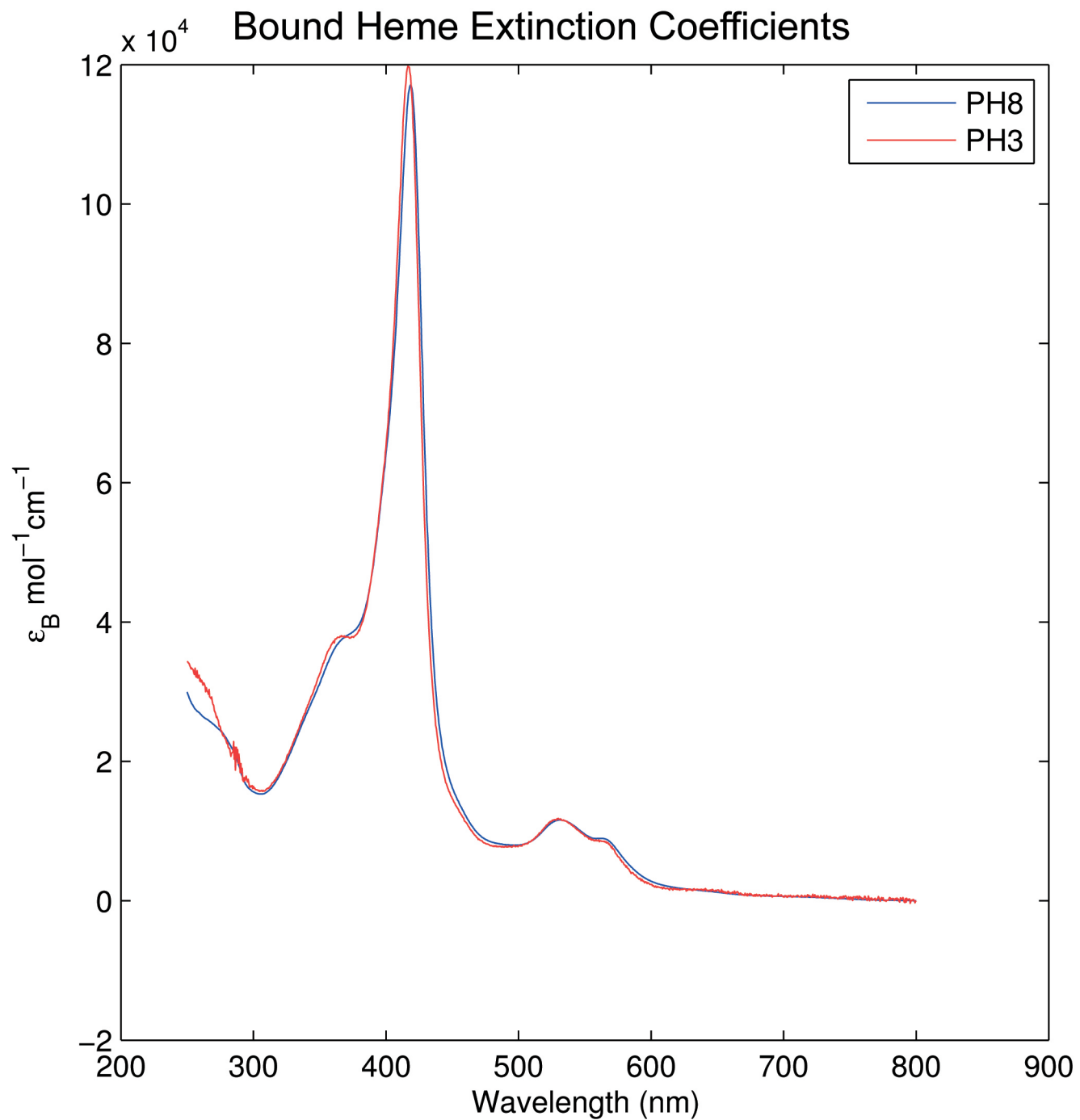


Figure 4: The extinction coefficients of bound heme in 0.1 M Tris HCl at pH 8 and 1 mM HCl at pH 3. This information is necessary to deconvolve the spectra arising from performing the heme titrations at pH 3. The acidic pH is required to keep the fibres intact.

## Measuring Parameters From TEM and AFM images

### AFM Measurements

Where possible, spatial measurements from the AFM data were made in such a way as to eliminate tip convolution errors. This is possible for  $L$  (whether high or low resolution data) by using a point at the same phase in each cycle (e.g. the distance between equivalent peaks in each cycle). The procedure for measuring  $D = 2R$  is demonstrated in Supporting Figure 5. If the sub-filaments can be resolved then the distance between the maxima of those filaments can be measured directly and this constitutes a convolution free estimate of the fibre width  $W$ . This is also direct confirmation of the existence of the filamentous nature of the fibre.

### TEM Measurements

The TEM was set up so that fibre samples, prepared with a negative stain as described in the methods and materials, were placed at the eucentric height and the goniometer tilt was set to zero, so that the image was projected orthogonally to the fibre axis and the magnification was reported faithfully. In such a case  $L$ ,  $R$  and  $\Delta Z$  are projected without distortion into a 2D image plane. In the spiral ribbon case  $W$  is distorted by a tiny proportion under projection,<sup>1</sup> depending on the amount of curvature remaining in the helical filament as it is adsorbed to the carbon film on the TEM grid. In the twisted ribbon case,  $W$  and  $R$  are effectively the same. Each measurement was made three times, using the techniques shown in Supporting Figure 6, and then averaged.



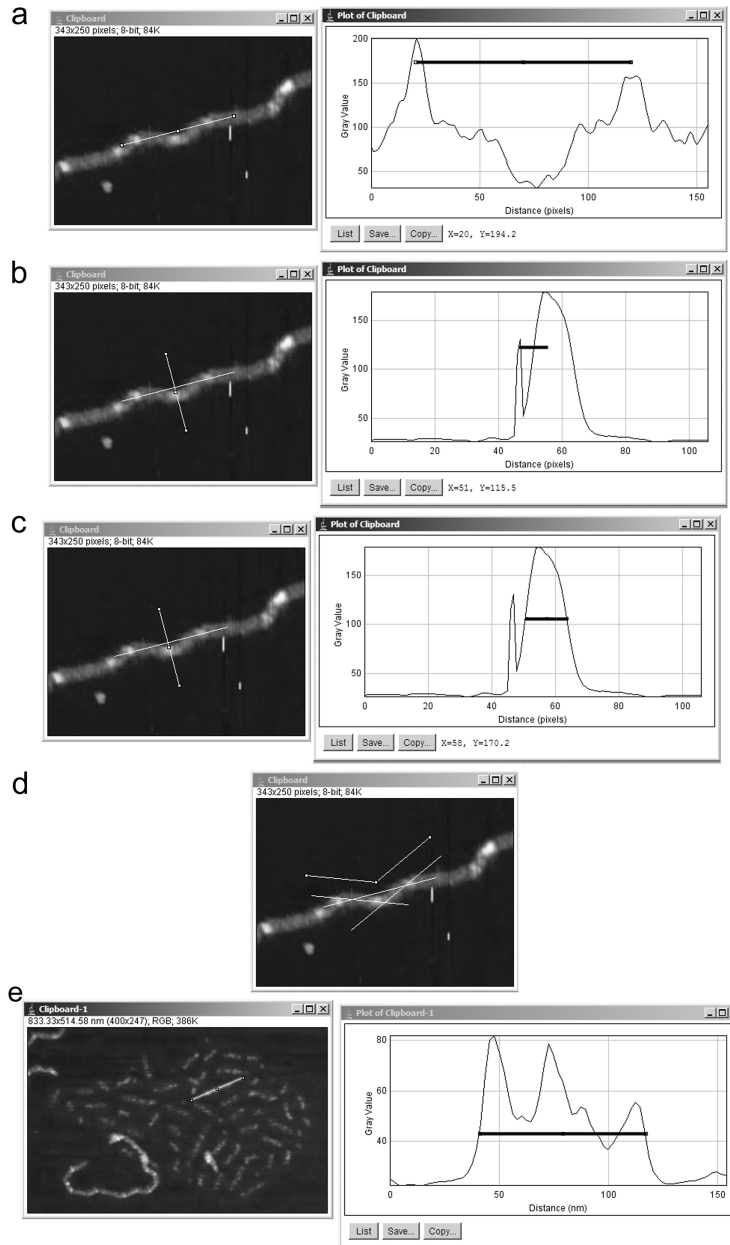


Figure 5: The parameters  $L$ ,  $D$ ,  $W$ ,  $\phi$  and  $F_l$  can all be measured from the AFM images. **a**: A convolution free measurement of  $L$  is obtained by drawing a profile through the two peaks defining the limits of a cycle. If desired, the height of the peak above the fibre can also be taken, which is usually twice the fibre height. **b**: The line is imprinted and a second perpendicular profile is taken. The diameter is taken as the distance from the line to the maximum of the fibre. This value will underestimate the diameter slightly. The alternative is to measure the tangential outer limits which will include tip convolution, thereby severely over-estimating the value. **c**: The full width half maximum of the fibre cross section can be measured as an estimate of the fibre width, which suffers from tip convolution. **d**: Two lines are drawn tangent to each segment and the angle between them measured with imageJ angle tool. **e**: The length of a fragment is measured as the full width half maximum of the longest axis.

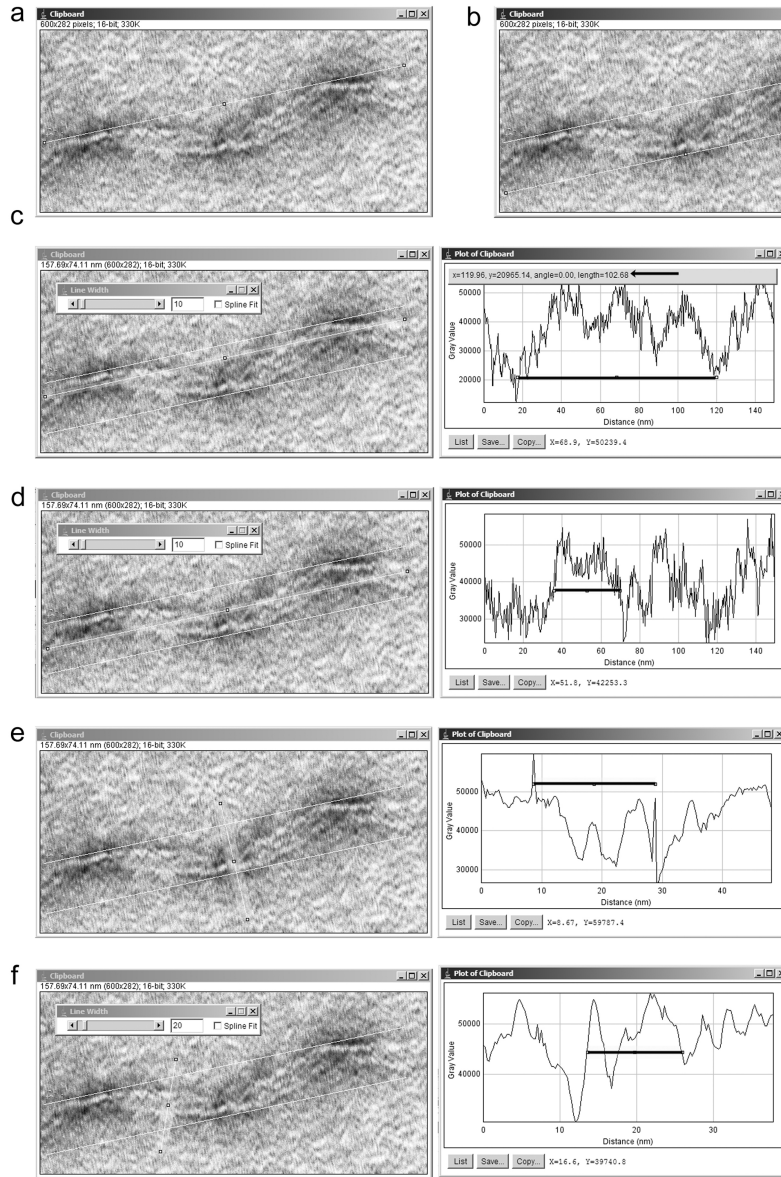


Figure 6: The parameters  $L$ ,  $D$ ,  $\Delta Z$  and  $W$ , can all be measured from TEM images. **a:** A 1px line is drawn that tangential to the outer limit of the adjacent cycles. The line is imprinted on the image and defines the axis of the cycle. **b:** The same profile is moved to be tangential to the extreme edge of the outer limit on the opposite side of the fibre and imprinted again. **c:** The line is expanded to 10px wide and moved to pass through the heavily stained regions where a profile can be used to measure  $L$  directly from the profile. **d:** The line is moved to be equidistant between the bounding imprints and a profile is taken to measure both  $\Delta Z$  values. **e:** A new line is drawn perpendicular to the fibre and the outer imprints are clearly visible in the profile, which defines the diameter  $D$ . **f:** The width of the fibre is measured with a profile perpendicular to the fibre.

## References

1. Forman, C. J. Towards the Control of the Morphology of Amyloid Fibrils Displaying Electron Transfer Proteins. Ph.D. thesis, University Of Cambridge, 2010.